

# Feasibility and stability in large Lotka Volterra systems with interaction structure

Xiaoyuan Liu<sup>1</sup>, George W.A. Constable, and Jonathan W. Pitchford  
*Department of Mathematics, University of York*

Complex system stability can be studied via linear stability analysis using Random Matrix Theory (RMT) or via feasibility (requiring positive equilibrium abundances). Both approaches highlight the importance of interaction structure. Here we show, analytically and numerically, how RMT and feasibility approaches can be complementary. In generalised Lotka-Volterra (GLV) models with random interaction matrices, feasibility increases when predator-prey interactions increase; increasing competition/mutualism has the opposite effect. These changes have crucial impact on the stability of the GLV model.

## I. INTRODUCTION

In the 1950s, ecologists such as Odum and MacArthur argued [1, 2] that ecosystems with a larger number of species tend to be more stable than less biodiverse systems. This idea was famously mathematised by May in 1972, who applied random matrix theory (RMT) to the problem [3]. May considered perturbations in  $n$  species abundances,  $\zeta$ , linearised about a hypothetical fixed point, with near-equilibrium dynamics described by

$$\frac{d\zeta}{dt} = A\zeta, \quad A_{ii} = -1, \quad A_{ij} = \sigma c a_{ij} \quad (1)$$

with  $a_{ij} \sim \mathcal{N}(0, 1)$  and  $c \sim B(1, C)$ . Here the diagonal elements of the matrix  $n \times n$  interaction matrix  $A$  represent self-regulation of the species, while its off-diagonal elements represent random species interactions that are non-zero with probability  $C$  (referred to as connectance) and when present have standard deviation  $\sigma$  (referred to as interaction strength). Since the asymptotic stability of Eq. (1) is governed solely by its eigenvalues, system-level stability is determined by characterising the eigenvalues of random matrix  $A$ .

The eigenvalue distribution of  $A$  is uniform across a circle in the complex plane, centered on  $(-1, 0)$  and with radius  $\sigma\sqrt{nC}$  as  $n \rightarrow \infty$  [3–5]. Thus the stability criterion for Eq. (1) is  $\sigma\sqrt{nC} < 1$  (see Fig. 1(a)). This suggests that more diverse ecosystems with more interspecific interactions are less likely to be stable for a given variance in interaction strength.

Allesina and Tang [6] added ecologically-motivated structure to May's approach, choosing elements of  $A$  pairwise by imposing a correlation,  $\rho$ , between  $a_{ij}$  and  $a_{ji}$  for  $j \neq i$  (e.g.  $(a_{ij}, a_{ji}) \sim \mathcal{N}(\mathbf{0}, \Sigma)$  with  $\Sigma = \sigma^2[(1, \rho), (\rho, 1)]$  [7]). Ecologically,  $\rho < 0$  implies more predator-prey interactions in the ecosystem, while  $\rho > 0$  implies more mutualistic and competitive interactions. Utilising another RMT result [8, 9] they generalised May's stability criterion to

$$\sigma\sqrt{nC}(1 + \rho) < 1. \quad (2)$$

Thus, increasing the proportion of predator-prey interactions increases stability, whilst increasing the proportion of competitive and mutualistic interactions reduces stability in Eq (1) (see Fig. 1(a)). Eq (2) implies that in the

extreme limit  $\rho \rightarrow -1$ , ecosystems are stable as long as there is self-regulation.

These analytic results are independent of the underlying non-linear model, but this apparent generality conceals an implicit assumption that the fixed point in (1) exists and is biologically meaningful. Such fixed points, where every species is present at a positive abundance, are termed feasible equilibria [10].

We use the generalised Lotka-Volterra model (GLV)

$$\frac{d\mathbf{x}}{dt} = \mathbf{x} \odot (\mathbf{r} + A\mathbf{x}), \quad (3)$$

to explore the links between Eq. (1) and feasibility. Here  $x_i$  is the abundance of species  $i$ ,  $r_i$  is its intrinsic growth rate,  $A$  the interaction matrix, and  $\odot$  the Hadamard product. Eq. (3) has a single non-zero fixed point,  $\mathbf{x}^*$ , with a Jacobian,  $J$ , such that

$$\mathbf{x}^* = -A^{-1}\mathbf{r}, \quad J = \mathbf{x}^*A \quad (4)$$

which is defined as feasible if  $x_i^* > 0 \forall i$ . The relationships between feasibility, stability and different system constraints such as interaction structure is a central theme in theoretical ecology [11]. Early analytic insight into the feasibility of  $\mathbf{x}^*$  in Eq. (4) assumed that  $A$  had interaction coefficients with fixed strengths, or with randomly generated signs [10, 12, 13]. Stone [14] linked this to May's approach by considering the probability that  $\mathbf{x}^*$  is feasible given an ensemble of interaction matrices constructed following Eq. (1) with uncorrelated  $a_{ij}$  [14]. Assuming that  $x_i^*$  is normally distributed for all  $i \in [1, n]$ , Stone showed that for a fully connected system  $C = 1$ , the probability of feasibility is

$$P_{\text{feas}} = 2^{-n} \left( 1 + \text{erf} \left( \frac{1}{\gamma_S \sqrt{1 + \gamma_S^2 + \gamma_S^4}} \right) \right)^n, \quad (5)$$

where  $\gamma_S = \sigma\sqrt{(n-1)}$  is known as the complexity in Stone's analysis. We see that  $P_{\text{feas}}$  drops sharply at a critical value of  $\gamma_S$ , and also has an additional dependence on system size  $n$  (see Fig. 1(b)). By working in the limit  $n \rightarrow \infty$ , [15, 16] determined a threshold interaction strength above which feasibility is lost in GLV systems with May type interaction matrices. An analytical prediction for the relationship between  $P_{\text{feas}}$  and the

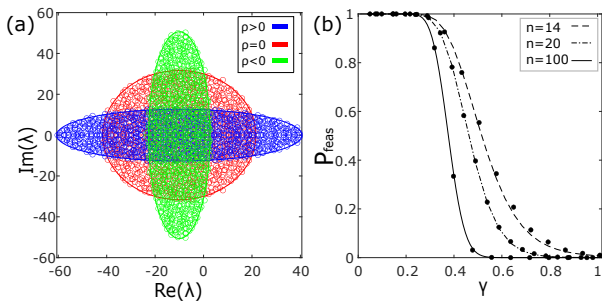


FIG. 1: (a) Eigenvalue distributions of interaction matrix  $A$  in (1) in which  $\text{Corr}(a_{ij}, a_{ji}) = \rho$ . Parameter values are  $\sigma = 1$ ,  $n = 1000$ ,  $C = 1$ ,  $|\rho| = 0.6$  and  $d = 10$ . (b) Feasibility probability  $P_{\text{feas}}$  as a function of complexity  $\gamma$  for an ensemble of random GLV systems ( $\rho = 0$ ) of community sizes ranging from  $n = 14$  to  $n = 100$ , reproduced from [14]. Curves are analytical predictions and markers are numerical simulations.

complexity  $\gamma = \sigma\sqrt{(n-1)C}$  which accounts for  $C$  was obtained by Dougoud et al. [17]. Akjouj et al. [18] investigated the feasibility of sparse ecosystems with interaction matrices that are block structured and  $d$ -regular (where each species interacts with  $d$  other species). Together these results suggest that feasibility is the more critical measure of complex system stability; compared to linear stability, feasibility is lost at smaller values of complexity. Here we seek to strengthen the links between RMT [3, 7] and feasibility analyses by calculating how the feasibility of an ecosystem changes with complexity [14, 17–19] when additional species interaction structure is added [6, 7]. It was shown by Bunin [11] that feasible systems lose stability above a certain interaction strength by transition to a phase with multiple attractors. The interaction strength of this phase transition increases as predator-prey interactions increase. Numerical results by Clenet et al. [15] also show that systems biased towards predator-prey interactions lose feasibility at larger interaction strengths than random systems, and those biased towards competition and mutualism lose feasibility at smaller interaction strengths. They also obtained an analytical result for the interaction strength above which feasibility is lost, in the limit of large  $n$  and without assessing the possible effect of  $\rho$ . To calculate  $P_{\text{feas}}$  in systems with such interaction structures, we must also obtain an approximation for the distribution of fixed points. This approximation opens up the possibility of leveraging recent results [20, 21] to determine the probability of stability of the GLV model with interaction structure.

## II. ANALYSIS

Following Stone [22] we obtain an analytic approximation of  $P_{\text{feas}}(\gamma)$  via the distribution of equilibrium species abundances  $P(\mathbf{x}^*)$ . By the Central limit theorem, we know that  $P(\mathbf{x}^*)$  is normal as  $n \rightarrow \infty$ , and that this

normality is a good approximation when  $n$  is large but finite. The task of calculating the feasibility probability is then equivalent to calculating

$$P_{\text{feas}} = \int_{\mathbf{x}^*=0}^{\infty} P(\mathbf{x}^*) d\mathbf{x}^* \approx \int_{\mathbf{x}^*=0}^{\infty} \mathcal{N}(\boldsymbol{\mu}_{\mathbf{x}^*}, \boldsymbol{\Sigma}_{\mathbf{x}^*}) d\mathbf{x}^* \quad (6)$$

where  $\boldsymbol{\mu}_{\mathbf{x}^*}$  and  $\boldsymbol{\Sigma}_{\mathbf{x}^*}$  are respectively the mean and covariance matrix of the species abundances at equilibrium.

We now calculate approximations for  $\boldsymbol{\mu}_{\mathbf{x}^*}$  and  $\boldsymbol{\Sigma}_{\mathbf{x}^*}$ . For simplicity we focus on the case  $r_i = 1 \forall i$  in Eq. (1). Recall that following [7], the elements of the interaction matrix  $a_{ij}$  and  $a_{ji}$  have correlation  $\rho$ . Writing  $A = \sigma\mathcal{E} - \mathbf{I}$ , our fixed point in Eq. (4) can be expressed as a Neumann series [23] for  $\|\sigma\mathcal{E}\| < 1$ :

$$\mathbf{x}^* = (\mathbf{I} - \sigma\mathcal{E})^{-1} \mathbf{r} \equiv \left( \sum_{j=0}^{\infty} (\sigma\mathcal{E})^j \right) \mathbf{r}. \quad (7)$$

This enables us, in principle, to calculate  $x_i^*$  up to an arbitrary order in  $\sigma$ . In our work, we approximate  $E(x_i^*)$ ,  $\text{Var}(x_i^*)$  and  $\text{Cov}(x_i^*, x_j^*)$  taking into account  $\rho$  and  $C$ . We approximate  $E(x_i^*)$  and  $\text{Cov}(x_i^*, x_j^*)$  up to order  $\sigma^3$ .

$$E(x_i^*) = 1 + (n-1)\rho C\sigma^2 + O(\sigma^4) \quad (8)$$

$$\text{Cov}(x_i^*, x_j^*) = \rho C\sigma^2 + O(\sigma^4) \quad (9)$$

Note, however, that feasibility is sensitive to the variance. It is therefore necessary to approximate the variance to a higher order in  $\sigma$  than  $E(x_i^*)$  and  $\text{Cov}(x_i^*, x_j^*)$ . Specifically, we approximate  $\text{Var}(x_i^*)$  to order  $\sigma^6$ . This approximation is given as follows.

$$\text{Var}(x_i^*) = (n-1)C\sigma^2 + c_4\sigma^4 + c_6\sigma^6 + O(\sigma^8) \quad (10)$$

where  $c_4$  and  $c_6$  are the coefficients of  $\sigma^4$  and  $\sigma^6$  respectively, which depend on  $n$ ,  $\rho$  and  $C$  (see Supplemental Material I.A and I.C). Specifically,  $c_4$  is the coefficient of  $\sigma^4$  in Eq. (S19) and  $c_6$  is obtained by subtracting Eq. (S29) from the expectation of Eq. (S28). The formulas for  $c_4$  and  $c_6$  are too lengthy to produce here, however of particular note is the fact that they are nontrivial polynomials that do not preserve the simple dependence on  $\gamma$ . Eq. (8) to Eq. (10) are then used to construct  $\boldsymbol{\mu}_{\mathbf{x}^*}$  and  $\boldsymbol{\Sigma}_{\mathbf{x}^*}$  in Eq. (6). To allow ease of computation for large systems, we reduced Eq. (6) to an expression involving a single integral, given by

$$P_{\text{feas}} = \int_{-\infty}^{\infty} \left\{ \prod_{i=1}^n \Phi\left(\frac{y_i - b_i u}{(1 - b_i^2)^{1/2}}\right) \right\} \phi(u) du \quad (11)$$

where  $\phi(u)$  is the density function of a standard normal random variable  $u$  and  $\Phi(v)$  denotes the cumulative distribution function of a standard normal random variable  $v$  [24]. In our analytical prediction of  $P_{\text{feas}}$ , we have that  $y_i = \frac{E(x_i^*)}{\sqrt{\text{Var}(x_i^*)}}$  and  $b_i = \frac{\sqrt{\text{Cov}(x_i^*, x_j^*)}}{\sqrt{\text{Var}(x_i^*)}}$ . In other words,

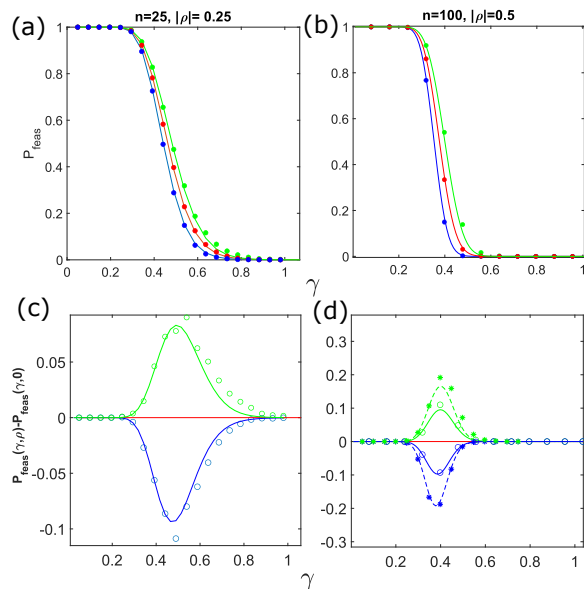


FIG. 2: Panels (a) and (b) plots the feasibility probability  $P_{\text{feas}}$  as a function of complexity  $\gamma$  for systems with ecologically motivated interaction structure. Numerical simulations (markers) are obtained as described in the Supplemental Material IV. (c) and (d) plots the difference between  $P_{\text{feas}}$  in systems with  $\rho \neq 0$  and  $P_{\text{feas}}$  in systems where  $\rho = 0$  ( $P_{\text{feas}}(\gamma, \rho) - P_{\text{feas}}(\gamma, 0)$ ) as a function of  $\gamma$ . Hollow circles and asterisks are numerical simulations for the case  $|\rho| = 0.25$  and  $|\rho| = 0.5$  respectively.

$P_{\text{feas}}$  is the expression obtained by substituting these expressions for  $y_i$  and  $b_i$  into (11). (see Supplemental Material III). Interestingly, note that in the results of [3, 7],  $C$  appears as a compound parameter with  $\sigma^2$ , but in Eq. (10)  $C$  would appear as a complicated polynomial form. The analytical prediction of  $P_{\text{feas}}(\gamma)$  is shown in Figure 2 (a)-(b).

## Results

### A. Predator-prey interactions increase the feasibility of random ecosystems

The qualitative difference in how  $P_{\text{feas}}$  changes with  $\gamma$  as  $\rho$  is varied is shown analytically in Figure 2. For a given value of  $n$ , when  $\rho > 0$  (blue) feasibility is lost at a smaller complexity compared to the case where  $\rho = 0$ . However when  $\rho < 0$ , we observe the opposite effect whereby feasibility is lost at a larger complexity than the case  $\rho = 0$ .

It can be seen in Figure 2 that the magnitude in the difference between  $P_{\text{feas}}(\gamma, \rho)$  and  $P_{\text{feas}}(\gamma, 0)$  also varies with  $\gamma$ . For instance when  $\gamma$  is sufficiently small, there is no difference between  $P_{\text{feas}}(\gamma, \rho)$  and  $P_{\text{feas}}(\gamma, 0)$  since  $P_{\text{feas}}$  is 1 regardless of  $\rho$ . The bottom panels of Figure 2 below plots this difference, demonstrating how it varies with  $\gamma$ . The difference between  $P_{\text{feas}}(\gamma, \rho)$  and  $P_{\text{feas}}(\gamma, 0)$

is the greatest for intermediate values of  $\gamma$ , where the system is transitioning rapidly away from feasibility. For a given system size  $n$ , the magnitude of this difference ( $|P_{\text{feas}}(\gamma, \rho) - P_{\text{feas}}(\gamma, 0)|$ ) also increases with the magnitude of  $\rho$ . When  $|\rho| = 0.5$ ,  $|P_{\text{feas}}(\gamma, \rho) - P_{\text{feas}}(\gamma, 0)|$  can be as large as 0.2 while for  $|\rho| = 0.25$ ,  $|P_{\text{feas}}(\gamma, \rho) - P_{\text{feas}}(\gamma, 0)|$  is at most 0.1 (see Figure 2).

In Supplemental Material I.D, we see that for all values of  $\rho$ , the loss of feasibility in the GLV model with Allesina and Tang type interaction matrices occurs at a smaller complexity than the loss of stability in the corresponding linear model. As an extreme example, in linear systems comprising all predator-prey interactions ( $\rho = -1$ ) stability is guaranteed regardless of ecosystem complexity (see Eq. (2)); conversely feasibility is still lost above a critical value of  $\gamma$  (see Figure S2 of Supplemental Material). Figure 2 demonstrates that the analytical results in Eq. (8) to Eq. (10) can be used to accurately predict  $P_{\text{feas}}$  as a function of  $\gamma$  in the case where  $C = 1$ . Furthermore, Supplemental Material V shows that the same analytical results remain highly accurate for predicting  $P_{\text{feas}}$  as a function of  $\gamma$  in the case where  $C = 0.3$ . By comparing the feasibility probabilities of such a system with that of a fully connected system, we see that a sparsely connected system of  $n = 100$  shows an almost identical feasibility-complexity relation as a fully connected system.

### B. Comparing RMT predictions with GLV Jacobian matrices

We have analytically approximated the distributions of  $x_i^*$  for non-linear GLV systems with interaction matrices constructed in the same manner as in the linear models of [7] (an interaction matrix  $A$  that accounts for  $\rho$  and  $C$ ). Having also determined the parameter regions of feasibility, we have the tools to allow us to determine the eigenvalue distribution of a feasible GLV Jacobian evaluated at equilibrium. Grilli et al. [20] studied the eigenvalue distribution of a matrix that is assumed to be of the same structure as the GLV Jacobian (Eq. (4)), where  $J$  is decomposed into a product of an interaction matrix  $A$  and fixed points  $\mathbf{x}^*$ . However, for simplicity, they assume that the distribution from which  $\mathbf{x}^*$  is drawn is independent of  $A$ , whereas this is clearly not the case (Eq. (4)).

Grilli's assumption of independence between the random elements of  $A$  and  $\mathbf{x}^*$  means that cross correlations between them need-not be considered, thereby simplifying the analysis. We test whether this assumption holds, in order to determine whether Grilli's method could be applicable to calculating the eigenvalue distribution of the GLV model with Allesina and Tang type interaction matrices. To do so, we calculate the eigenvalue distribution of  $J = \mathbf{x}^* A$  where the elements of  $\mathbf{x}^*$  are sampled independently to those of  $A$ . We then compare this eigenvalue distribution to that of the GLV Jacobian where the exact  $\mathbf{x}^*$  corresponding to each given  $A$  is used.

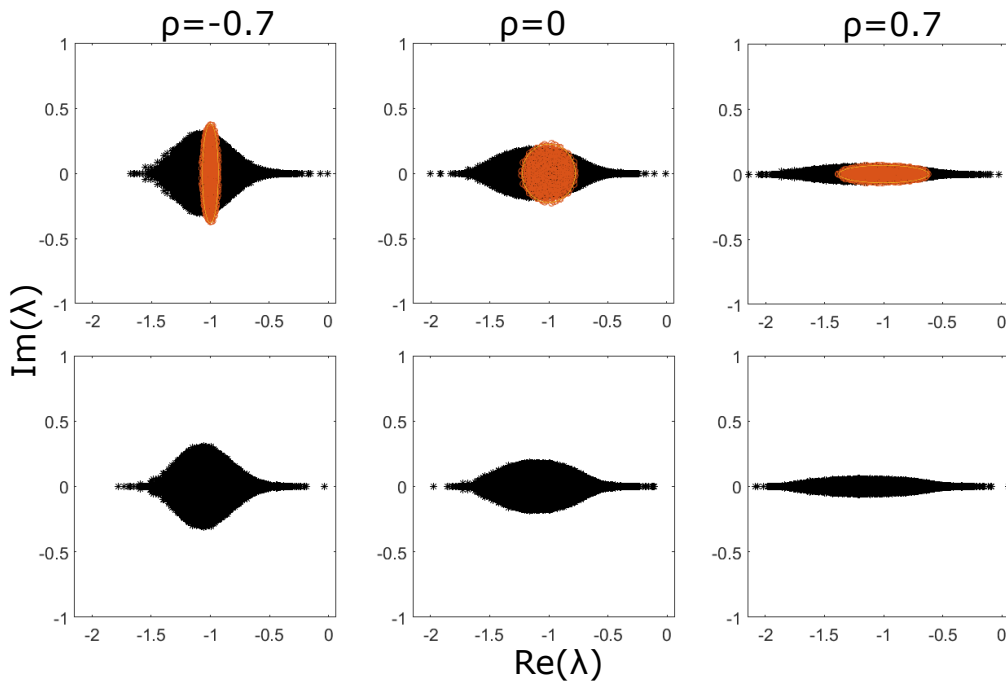


FIG. 3: Top row: Orange ellipses are eigenvalue distributions of  $A$  with  $\rho$  specified above the panels. Yellow boundaries are predicted by Allesina and Tang. Black markers represent 50 realisations of the eigenvalue distribution of the GLV Jacobian  $J = \mathbf{x}^* A$  where the exact  $\mathbf{x}^*$  corresponding to each given  $A$  is used. Bottom row: 50 realisations of the eigenvalue distribution of  $J = \mathbf{x}^* A$  where elements of  $\mathbf{x}^*$  are sampled independently of the random variables in  $A$ , from the multivariate normal distribution determined by parameters  $n$ ,  $\rho$ ,  $\sigma$  and  $C$  of  $A$  (see Eqs.(8-10)).  $Var(x_i^*)$  is approximated up to and including  $\sigma^6$ . Parameter values are  $\sigma = 0.01$ ,  $n = 500$  and  $C = 1$ . For the left panel  $P_{\text{feas}} = 0.993$ , middle panel  $P_{\text{feas}} = 0.997$  and right panel  $P_{\text{feas}} = 1.000$ .

The black markers on the top panels of Figure 3 show the eigenvalue distributions of the Jacobian  $J = \mathbf{x}^* A$  where the exact  $\mathbf{x}^*$  corresponding to each given  $A$  is used. By comparing the black markers on the top panels with those of the bottom panels, we see that the method of sampling  $\mathbf{x}^*$  from our distribution of  $\mathbf{x}^*$  (independently of  $A$ ) to construct  $J$  works well in regions where feasibility is guaranteed. From the top panels, we see that for  $\rho < 0$ , the bulk eigenvalue distribution of  $J$  gets stretched in the  $Im(\lambda)$  plane, and for  $\rho > 0$  in the  $Re(\lambda)$  plane. This qualitative effect is consistent with the result of Allesina and Tang [7]. It is shown numerically in Supplemental Material VI that increasing  $\rho$  decreases the average resilience and probability of stability of the GLV model.

The average maximum outlier eigenvalue is also correctly predicted by our theory, which relies on the assumption of statistical independence between  $A$  and our calculated distribution of  $\mathbf{x}^*$  (see Eqs.(8-10)), as illustrated in Figure S6 (a). However, we note that as can be seen from Figure 3, it fails to capture the maximum outlier eigenvalue observed over multiple realisations. This suggests that cross-correlations between the entries of  $A$  and  $\mathbf{x}^*$  may be quantitatively important in calculating the stability of a GLV system for individual realisations. As the stability of a system is governed solely by the eigenvalue with the largest real part, a stability analysis

of the GLV model must be preceded by means of calculating such an eigenvalue. Below, we provide an insight into some possible techniques for calculating the stability of the GLV system.

Stone [19] showed that provided that  $\|\sigma\mathcal{E}\|$  is sufficiently small, the eigenvalue with the largest real part (outlier eigenvalue of  $J$ ) is approximately equal to minus the abundance of the least abundant species i.e  $\lambda_{max} \approx -\min_{i \in \{1, n\}} x_i^*$ ; in which case we have the weak condition whereby feasibility corresponds to the local asymptotic stability of the GLV system. In the case where  $\rho = 0$  or  $|\rho|$  is small,  $-\min_{i \in \{1, n\}} x_i^*$  is an accurate estimate of the outlier eigenvalue of  $J$ , however this accuracy breaks down as we increase  $|\rho|$  (see Supplemental Material VI). Relying on Grilli's assumption allows us to accurately capture the bulk eigenvalue distribution of  $J$  and the effect of  $\rho$  on the average stability over a large number of realisations, although it fails to accurately calculate the outlier eigenvalue of  $J$  corresponding to a specific realisation of  $A$ .

## Discussion

We have obtained an analytical prediction of the feasibility probability as a function of complexity  $\gamma =$

$\sigma\sqrt{(n-1)C}$  for random GLV systems with interaction matrices of Allesina and Tang type [7]. By extending the analytical result of [15] to the case of finite  $n$ , we have shown that a positive value of  $\rho$  reduces the feasibility probability for a given complexity, while a negative value of  $\rho$  increases the corresponding feasibility probability, an effect not quantifiable in the infinite  $n$  limit. We have also accounted for the connectance  $C$ . Since natural ecological systems are sparsely connected [25], both these generalisations mentioned above add biological realism to the result of Stone 2016 [22]. Relationships between complexity and feasibility have also been studied by [26], where they characterised feasibility by how freely one could choose the intrinsic growth rate vectors to allow the system to remain feasible. As a whole, these results strengthen connections between feasibility and RMT systems, whilst also adding biological realism.

Along the way, we managed to analytically approximate the distribution of  $\mathbf{x}^*$  as a function of the system parameters  $n$ ,  $C$ ,  $\sigma$  and  $\rho$ . This has allowed us to check the utility of Grilli’s assumption of independence between  $\mathbf{x}^*$  and  $A$  in predicting the eigenvalue distribution of the Jacobian of GLV systems with Allesina and Tang type interaction matrices [19, 20]. Figure 3 shows that Grilli’s assumption can be relied upon to accurately predict the effect of interaction structure [7] on the eigenvalue distribution of feasible random GLV systems. However, relying on this assumption does not allow us to reliably calculate the outlier eigenvalue of the GLV Jacobian of a particular realisation.

It is of note that our method for calculating the feasibility probability relies on several assumptions on the parameter values to ensure accuracy (see Supplemental Material I.D and II). We also assumed that  $x_i^*$  is normally distributed. Since the Neumann series approximation for  $x_i^*$  is normal in the limit  $n \rightarrow \infty$ , and is convergent if and only if  $\sigma\sqrt{nC} < 1$ , our method is accurate for large  $n$  and small  $\sigma$  (see Supplemental Material II). Since the Neumann series expansion is precise, it is straightforward to extend our analysis to arbitrary orders of precision by working to higher orders in  $\sigma$  (see Eq.(7)).

The concept of feasibility has been associated with the extinction probability. It was summarised by Stone 1988 [14] that a higher feasibility probability is linked

to the reduction in the probability of extinction following structural disturbances, which are changes in interaction strengths caused by environmental change. Our results imply that increasing predator-prey interactions reduces the chance of extinction following structural disturbances.

We have used the assumption of May 1972 that all species are self-regulating. This is representative of natural ecosystems since ecosystems would require 50 percent of species to self-regulate to allow for stability [27]. However, the assumption that  $r_i = 1 \forall i \in [1, n]$  may not be biologically realistic, as natural ecosystems contain consumer species which do not grow in isolation. This is an interesting area for future investigation, however it was suggested by Song et al [28] that this assumption gives the parameter region where feasible systems are likely to be present.

Having generalised the distribution of  $\mathbf{x}^*$  to account for arbitrary  $\rho$ , we have opened up the possibility for extending the results of Grilli et al. [20] to analytically predict the boundary of the eigenvalue distribution of the GLV Jacobian of such systems. This analytical prediction would enable us to calculate the stability of such GLV systems. One potential method to perform this calculation is by applying the cavity method as detailed in [20]. It may also be possible to calculate the expected value of  $-\min_{i \in \{1, n\}} x_i^*$  by applying order statistics as detailed in [29], and thus the expected resilience of a GLV system with a given value of  $\rho$ , although this is only applicable to systems where  $|\rho|$  is small. Overall, our analyses, combined with [7, 15, 29] manifest that increasing the proportion of predator-prey interactions not only increases feasibility, but also the resilience of feasible GLV systems. This provides greater support to Allesina and Tang’s [7] conclusion that predator-prey interactions are stabilising whilst competitive/mutualistic interactions are destabilising.

## Acknowledgments

We thank the Complexity and Stability reading group at the University of York for useful discussions.

- 
- [1] Eugene P Odum. Fundamentals of ecology (1953). In *The Future of Nature*, pages 233–244. Yale University Press, 2013.
  - [2] Robert MacArthur. Fluctuations of animal populations and a measure of community stability. *ecology*, 36(3):533–536, 1955.
  - [3] Robert M May. Will a large complex system be stable? *Nature*, 238(5364):413–414, 1972.
  - [4] Eugene P. Wigner. On the distribution of the roots of certain symmetric matrices. *The Annals of Mathematics*, 67(2):325, 1958.
  - [5] Terence Tao, Van Vu, and Manjunath Krishnapur. Random matrices: Universality of esds and the circular law. *The Annals of Probability*, 38(5):2023–2065, 2010.
  - [6] Stefano Allesina and Si Tang. Stability criteria for complex ecosystems. *Nature*, 483(7388):205–208, 2012.
  - [7] Stefano Allesina and Si Tang. The stability–complexity relationship at age 40: a random matrix perspective. *Population Ecology*, 57(1):63–75, 2015.
  - [8] VL Girko. Elliptic law. *Theory of Probability & Its Applications*, 30(4):677–690, 1986.
  - [9] Hans Juergen Sommers, Andrea Crisanti, Haim Som-

- polinsky, and Yaakov Stein. Spectrum of large random asymmetric matrices. *Physical review letters*, 60(19):1895, 1988.
- [10] Alan Roberts. The stability of a feasible random ecosystem. *Nature*, 251(5476):607–608, 1974.
- [11] Guy Bunin. Ecological communities with lotka-volterra dynamics. *Physical Review E*, 95(4):042414, 2017.
- [12] Michael E Gilpin. Stability of feasible predator-prey systems. *Nature*, 254(5496):137–139, 1975.
- [13] BS Goh and LS Jennings. Feasibility and stability in randomly assembled lotka-volterra models. *Ecological Modelling*, 3(1):63–71, 1977.
- [14] Lewi Stone. *Some problems of community ecology: processes, patterns and species persistence in ecosystems*. PhD thesis, Monash University, 1988.
- [15] Maxime Clenet, E Ferchichi, and Jamal Najim. Equilibrium in a large lotka-volterra system with pairwise correlated interactions. *arXiv preprint arXiv:2205.15591*, 2022.
- [16] Pierre Bizeul and Jamal Najim. Positive solutions for large random linear systems. *Proceedings of the American Mathematical Society*, 149(6):2333–2348, 2021.
- [17] Michaël Dougoud, Laura Vinckenbosch, Rudolf P Rohr, Louis-Félix Bersier, and Christian Mazza. The feasibility of equilibria in large ecosystems: A primary but neglected concept in the complexity-stability debate. *PLoS computational biology*, 14(2):e1005988, 2018.
- [18] Imane Akjouj and Jamal Najim. Feasibility of sparse large lotka-volterra ecosystems. *arXiv preprint arXiv:2111.11247*, 2021.
- [19] Lewi Stone. The feasibility and stability of large complex biological networks: a random matrix approach. *Scientific reports*, 8(1):1–12, 2018.
- [20] Theo Gibbs, Jacopo Grilli, Tim Rogers, and Stefano Allesina. Effect of population abundances on the stability of large random ecosystems. *Physical Review E*, 98(2), 2018.
- [21] Joseph W Baron, Thomas Jun Jewell, Christopher Ryder, and Tobias Galla. Eigenvalues of random matrices with generalized correlations: A path integral approach. *Physical Review Letters*, 128(12):120601, 2022.
- [22] Lewi Stone. The google matrix controls the stability of structured ecological and biological networks. *Nature communications*, 7(1):1–7, 2016.
- [23] Rainer Kress. *Linear integral equations*. Springer, 2014.
- [24] Robert N Curnow and Charles W Dunnett. The numerical evaluation of certain multivariate normal integrals. *The Annals of Mathematical Statistics*, pages 571–579, 1962.
- [25] Mark R Gardner and W Ross Ashby. Connectance of large dynamic (cybernetic) systems: critical values for stability. *Nature*, 228(5273):784–784, 1970.
- [26] Jacopo Grilli, Matteo Adorisio, Samir Suweis, György Barabás, Jayanth R Banavar, Stefano Allesina, and Amos Maritan. Feasibility and coexistence of large ecological communities. *Nature communications*, 8(1):1–8, 2017.
- [27] György Barabás, Matthew J Michalska-Smith, and Stefano Allesina. Self-regulation and the stability of large ecological networks. *Nature ecology & evolution*, 1(12):1870–1875, 2017.
- [28] Chuliang Song and Serguei Saavedra. Will a small randomly assembled community be feasible and stable? *Ecology*, 99(3):743–751, 2018.
- [29] Susanne Pettersson, Van M Savage, and Martin Nilsson Jacobi. Predicting collapse of complex ecological systems: quantifying the stability–complexity continuum. *Journal of the Royal Society Interface*, 17(166):20190391, 2020.

# Supplemental Material: Feasibility and Stability in Large Lotka-Volterra systems with interaction structure

Xiaoyuan Liu<sup>1</sup>, George W.A. Constable, and Jonathan W. Pitchford<sup>1</sup>

<sup>1</sup>*Department of Mathematics, University of York*

(Dated: August 2022)

arXiv:2211.12949v1 [q-bio.PE] 23 Nov 2022

# I. ANALYTICALLY APPROXIMATING $Var(x_i^*)$ TO ORDER $\sigma^6$

## A. Coefficient of $\sigma^4$ in $Var(x_i^*)$

We first approximate the coefficient of  $\sigma^4$  in  $Var(x_i^*)$ . To do this we specify the Taylor expansion of  $x_i^*$  in  $\sigma$  in index notation. In matrix form, the Taylor expansion of  $\mathbf{x}^*$  to order  $\sigma^4$  is

$$\mathbf{x}^* = (\mathbf{I} + \sigma\mathcal{E} + \sigma^2\mathcal{E}^2 + \sigma^3\mathcal{E}^3 + \sigma^4\mathcal{E}^4 + O(\sigma^5))\mathbf{r} \quad (\text{S1})$$

where

$$\mathcal{E} = \begin{pmatrix} 0 & a_{12} & \dots & a_{1n} \\ & \ddots & & \\ & & 0 & \\ a_{n1} & & & 0 \end{pmatrix}, \quad \mathbf{r} = \begin{bmatrix} 1 \\ 1 \\ \vdots \\ 1 \end{bmatrix} \quad (\text{S2})$$

In index notation, (S1) can be expressed as

$$x_i^* = 1 + \sigma\mathcal{E}_{ij} + \sigma^2(\mathcal{E}^2)_{ij} + \sigma^3(\mathcal{E}^3)_{ij} + \sigma^4(\mathcal{E}^4)_{ij} + O(\sigma^5) \quad (\text{S3})$$

since  $r_i = 1$  for all  $i \in [1, n]$ . All terms in (S3) represent terms to be summed over. The subscript  $i$  in (S3) is the free index while all other indices are dummy indices. Please note that terms such as  $\mathcal{E}_{ij}$  denote vectors and not matrices, since  $i$  is the free index.  $Var(x_i^*)$  is defined by the equation

$$Var(x_i^*) = E(x_i^{*2}) - E(x_i^*)^2 \quad (\text{S4})$$

so we need to we seek the second moment of  $x_i^*$ , which can be found using (S3). The expression for  $x_i^{*2}$  is deduced by squaring (S3). Since the expectation of all terms of odd powers of  $\sigma$  is 0, we can safely ignore them, which gives

$$x_i^{*2} = 1 + \sigma^2(2(\mathcal{E}^2)_{ij} + \mathcal{E}_{ij}\mathcal{E}_{ik}) + \sigma^4(2(\mathcal{E}^4)_{ij} + 2(\mathcal{E}^3)_{ij}(\mathcal{E})_{ik} + (\mathcal{E}^2)_{ij}(\mathcal{E}^2)_{ik}) + O(\sigma^6) \quad (\text{S5})$$

which we can apply to calculate the second moment of  $x_i^*$ . We see from (S5) that we need to determine  $E((\mathcal{E}^4)_{ij})$ ,  $E((\mathcal{E}^3)_{ij}(\mathcal{E})_{ik})$  and  $E((\mathcal{E}^2)_{ij}(\mathcal{E}^2)_{ik})$ . The expression for  $(\mathcal{E}^4)_{im}$  can be expressed as a sum of terms involving products of interaction coefficients

$$(\mathcal{E}^4)_{im} = \sum_{k=1}^n \sum_{j \neq i, j \neq k}^n \sum_{l \neq k, l \neq m}^n a_{ij}a_{jk}a_{kl}a_{lm} \quad (\text{S6})$$

and the expression for  $(\mathcal{E}^4)_{ij}$  is

$$(\mathcal{E}^4)_{ij} = (\mathcal{E}^4)_{ii} + (\mathcal{E}^4)_{ij}\mathbf{1}_{\{j \neq i\}} \quad (\text{S7})$$

we first determine the expectation of  $(\mathcal{E}^4)_{ii}r_i$ . We see from (S6) that the expression for  $(\mathcal{E}^4)_{ii}$  is

$$(\mathcal{E}^4)_{ii} = \sum_{k=1}^n \sum_{j \neq i, j \neq k}^n \sum_{l \neq k}^n a_{ij}a_{jk}a_{kl}a_{li} \quad (\text{S8})$$

It is also possible for (S8) to have terms where  $i = k$ ,  $j = l$  or both, which give rise to terms of (S8) with nonzero expectation. To represent the case where  $i = k$  but  $j \neq l$ , (S8) is multiplied by  $\delta_{ik}$  and to represent the case where  $j = l$  but  $i \neq k$ , (S8) is multiplied by  $\delta_{jl}$ . To represent the case where both  $i = k$  and  $j = l$ , we multiply (S8) by  $\delta_{ik}\delta_{jl}$ . The expectation of (S8) is

$$E((\mathcal{E}^4)_{ii}) = E\left(\sum_{k=1}^n \sum_{j \neq i, j \neq k}^n \sum_{l \neq k}^n a_{ij}a_{jk}a_{kl}a_{li}(\delta_{ik} + \delta_{jl} + \delta_{ik}\delta_{jl})\right) \quad (\text{S9})$$

$$\begin{aligned} &= \sum_{j \neq i, j \neq l}^n \sum_{l \neq i}^n E(a_{ij}a_{ji}a_{il}a_{li}) + \sum_{j \neq i}^n \sum_{k \neq j, k \neq i}^n E(a_{ij}a_{jk}a_{kj}a_{ji}) + \sum_{j \neq i}^n E(a_{ij}^2 a_{ji}^2) \\ &= (n-1)(1 + 2(n-1)\rho^2) \end{aligned} \quad (\text{S10})$$



It is also proven in Section IB below that the second summation term of (S7)  $(\mathcal{E}^4)_{ij}\mathbf{1}_{\{j \neq i\}}$  has an expectation of 0, which implies that

$$\begin{aligned} E((\mathcal{E}^4)_{ij}) &= E((\mathcal{E}^4)_{ii}) \\ &= 2(n-1)(n-2)\rho^2 + (n-1)(1+2\rho^2) \\ &= (n-1)(1+2(n-1)\rho^2) \end{aligned} \quad (\text{S11})$$

The expression for  $(\mathcal{E}^3)_{ij}\mathcal{E}_{ik}$  can be expressed as a sum of terms involving products of interaction coefficients

$$(\mathcal{E}^3)_{ij}\mathcal{E}_{ik} = \sum_{k=1}^n \sum_{j \neq i, j \neq k}^n \sum_{l \neq k, l \neq m}^n a_{ij}a_{ik}a_{kl}a_{lm} \quad (\text{S12})$$

The terms that give rise to nonzero expectation of (S12) include those where  $m = k$  and  $i = l$ ,  $l = i$  and  $m = j$  and those where  $m = k$  only.

$$\begin{aligned} E((\mathcal{E}^3)_{ij}\mathcal{E}_{ik}) &= E\left(\sum_{k=1}^n \sum_{j \neq i, j \neq k}^n \sum_{l \neq k}^n a_{ij}a_{ik}a_{kl}a_{lm}(\delta_{il}\delta_{mk} + \delta_{il}\delta_{mj} + \delta_{mk})\right) \\ &= \sum_{j \neq i, j \neq l}^n \sum_{l \neq i}^n E(a_{ij}^2 a_{ik} a_{ki}) + \sum_{j \neq i}^n \sum_{k \neq j, k \neq i}^n E(a_{ik}^3 a_{ki}) + \sum_{j \neq i}^n E(a_{ik}^2 a_{kl} a_{lk}) \\ &= 3(n-1)\rho + 2(n-1)(n-2)\rho \end{aligned} \quad (\text{S13})$$

The expression for  $(\mathcal{E}^2)_{ij}(\mathcal{E}^2)_{ik}$  can be expressed as a sum of terms involving products of interaction coefficients

$$(\mathcal{E}^2)_{ij}(\mathcal{E}^2)_{ik} = \sum_{k=1}^n \sum_{j \neq i, j \neq k}^n \sum_{l \neq k, l \neq m}^n a_{ij}a_{jk}a_{il}a_{lm} \quad (\text{S15})$$

The terms that give rise to nonzero expectation of (S15) include those where  $k = i$  and  $l = j$  and  $m = i$ ,  $k = m$  and  $j = l$  and those where  $k = i$  and  $m = i$ .

$$\begin{aligned} E((\mathcal{E}^2)_{ij}(\mathcal{E}^2)_{ik}) &= E\left(\sum_{k=1}^n \sum_{j \neq i, j \neq k}^n \sum_{l \neq k}^n a_{ij}a_{jk}a_{il}a_{lm}(\delta_{ki}\delta_{lj}\delta_{mi} + \delta_{km}\delta_{jl} + \delta_{ki}\delta_{mi})\right) \\ &= \sum_{j \neq i, j \neq l}^n \sum_{l \neq i}^n E(a_{ij}^2 a_{ji}^2) + \sum_{j \neq i}^n \sum_{k \neq j, k \neq i}^n E(a_{ij}^2 a_{jk}^2) + \sum_{j \neq i}^n E(a_{ij}a_{ji}a_{il}a_{li}) \\ &= (n-1)((n-1) + n\rho^2) \end{aligned} \quad (\text{S16})$$

We have also ensured that no terms in all the summations above are double counted. Substituting all the results derived here into (S5), we see that the coefficient of  $Var(x_i^*)$  at order  $\sigma^4$  is  $(n-1)^2 + \rho(n-1)(4n-2) + \rho^2(n-1)$ , and combined with the coefficient of  $Var(x_i^*)$  at order  $\sigma^2$  we get

$$Var(x_i^*) = (n-1)\sigma^2 + \sigma^4 \left( (n-1)^2 + \rho(n-1)(4n-2) + \rho^2(n-1) \right) + O(\sigma^6) \quad (\text{S18})$$

We can generalise the expression for  $Var(x_i^*)$  to account for the connectance  $C$ . Since  $a_{ij}$  and  $a_{ji}$  are zero with probability  $(1-C)$  and are sampled from a bivariate normal distribution with probability  $C$  and  $Corr(a_{ij}, a_{ji}) = \rho$ , we have that

$$\begin{aligned} Var(x_i^*) &= (n-1)C\sigma^2 + \sigma^4 \left( [C(n-1) + C^2(n-1)(n-2)] + \rho[4C^2(n-1)(n-2) + 6C(n-1)] + \right. \\ &\quad \left. \rho^2[2C(n-1) + C^2(n-1)(n-2) - (n-1)^2C^2] \right) + O(\sigma^6) \end{aligned} \quad (\text{S19})$$

The analytics in (S19) show that for the case where  $C < 1$ , sampling  $a_{ij}$  and  $a_{ji}$  from a bivariate distribution with probability  $C$  gives a different  $Var(x_i^*)$  to when  $A$  is sampled randomly with connectance  $C$ , as was done by May [1].

### B. Proof that $\sum_{j \neq i}^n (\mathcal{E}^4)_{ij} r_j$ has Zero Expectation

In the particular scenario where  $i \neq m$  in (S6), the possible scenarios are  $m = j$ ,  $m = k$  and  $m = l$ . In the case where  $m = j$ , (S6) becomes

$$(\mathcal{E}^4)_{ij} = \sum_{k=1}^n \sum_{j \neq i, j \neq k}^n \sum_{l \neq k, l \neq j}^n a_{ij} a_{jk} a_{kl} a_{lj} \quad (\text{S20})$$

and it is possible that  $i = k$ ,  $j = l$  or  $i = l$ . If  $j = l$ , (S20) is 0 since  $\mathcal{E}_{ii} = 0$  for all  $i \in [1, n]$ . We therefore consider the cases  $i = l$  and  $i = k$  in the case where  $m = j$ . The expression for the expectation of  $(\mathcal{E}^4)_{ij}$  is

$$\begin{aligned} E((\mathcal{E}^4)_{ij}) &= E\left(\sum_{k=1}^n \sum_{j \neq i, j \neq k}^n \sum_{l \neq k}^n a_{ij} a_{jk} a_{kl} a_{lj} (\delta_{ik} + \delta_{il} + \delta_{ik} \delta_{il})\right) \\ &= \sum_{j \neq i, j \neq l} \sum_{l \neq i} E(a_{ij} a_{jk} a_{kl} a_{lj}) + \sum_{j \neq i} \sum_{k \neq j, k \neq i} E(a_{ij} a_{jk} a_{ki} a_{ij}) + 0 \\ &= 0 \end{aligned} \quad (\text{S21})$$

Now we consider the case where  $m = k$ . In this case, it is possible that  $j = l$  and  $i = l$ . It is not possible for  $i = k$  since we are considering the scenario in (S6) where  $i \neq m$ . The expression for the expectation of  $(\mathcal{E}^4)_{ik}$  is

$$\begin{aligned} E((\mathcal{E}^4)_{ik}) &= E\left(\sum_{k=1}^n \sum_{j \neq i, j \neq k}^n \sum_{l \neq k}^n a_{ij} a_{jk} a_{kl} a_{lk} (\delta_{il} + \delta_{jl} + \delta_{jl} \delta_{il})\right) \\ &= \sum_{j \neq i, j \neq l} \sum_{l \neq i} E(a_{ij} a_{jk} a_{kl} a_{lk}) + \sum_{j \neq i} \sum_{k \neq j, k \neq i} E(a_{ij} a_{jk} a_{kj} a_{jk}) + 0 \\ &= 0 \end{aligned} \quad (\text{S24})$$

Finally, in the case where  $m = l$ , we have that  $E((\mathcal{E}^4)_{il}) = 0$  since  $(\mathcal{E}^4)_{il}$  involves a product of  $\mathcal{E}_{lm}$  which equals 0 if  $l = m$ . We have therefore proven that  $\sum_{j \neq i}^n (\mathcal{E}^4)_{ij} r_j$  has an expectation of 0.

### C. Coefficient of $\sigma^6$ in $Var(x_i^*)$

To obtain the coefficient of  $\sigma^6$  in  $Var(x_i^*)$ , we apply the Taylor expansion of  $x_i^*$  up to order  $\sigma^6$ , given by

$$\mathbf{x}^* = (\mathbf{I} + \sigma \mathcal{E} + \sigma^2 \mathcal{E}^2 + \sigma^3 \mathcal{E}^3 + \sigma^4 \mathcal{E}^4 + \sigma^5 \mathcal{E}^5 + \sigma^6 \mathcal{E}^6 + O(\sigma^7)) \mathbf{r} \quad (\text{S25})$$

which in index notation is

$$x_i^* = 1 + \sigma \mathcal{E}_{ij} + \sigma^2 (\mathcal{E}^2)_{ij} + \sigma^3 (\mathcal{E}^3)_{ij} + \sigma^4 (\mathcal{E}^4)_{ij} + \sigma^5 (\mathcal{E}^5)_{ij} + \sigma^6 (\mathcal{E}^6)_{ij} + O(\sigma^7) \quad (\text{S26})$$

Again, we need to apply (S4), which requires us to calculate the second moment of  $x_i^*$  as well as  $E(x_i^*)^2$ . To calculate  $E(x_i^*)$ , we need to calculate  $E((\mathcal{E}^6)_{ij})$ . To calculate  $E(x_i^*)^2$ , we need to calculate the expectation of the square of (S26) with terms of order higher than  $\sigma^6$  truncated. At order  $\sigma^6$ , it is convenient to adopt a different notation to that detailed in Section I. Here, we re-express the matrix  $\mathcal{E}$  in the form

$$\mathcal{E} = \sum_{i=1}^{n-1} \sum_{j=2, j>i}^n \Phi_{ij} \quad (\text{S27})$$

where  $\Phi_{ij}$  represents matrices such that their  $(i, j)$ -th component is  $a_{ij}$  (i.e.  $(\Phi_{ij})_{ij} = a_{ij}$  and  $(\Phi_{ij})_{ji} = a_{ji}$  for  $j > i$ ) and all other entries are zero. The coefficients of  $x_i^*{}^2$  at order  $\sigma^6$  are given in (S28) below.

$$2(\mathcal{E}^6)_{ij} + 2(\mathcal{E}^5)_{ij} \mathcal{E}_{ik} + 2(\mathcal{E}^4)_{ij} (\mathcal{E}^2)_{ik} + (\mathcal{E}^3)_{ij} (\mathcal{E}^3)_{ik} \quad (\text{S28})$$

and the coefficients of  $Var(x_i^*)$  at order  $\sigma^6$  of  $E(x_i^*)^2$  are

$$2E[(\mathcal{E}^6)_{ij}] + 2E[(\mathcal{E}^4)_{ii}]E[(\mathcal{E}^2)_{ii}] \quad (\text{S29})$$

The coefficient of  $\sigma^6$  in  $Var(x_i^*)$  can be deduced simply by subtracting (S29) from the expectation of (S28). To calculate the coefficient of  $\sigma^6$  in  $Var(x_i^*)$ , it is necessary to calculate the expectation of  $(\mathcal{E}^6)_{ij}$ ,  $(\mathcal{E}^5)_{ij}(\mathcal{E})_{ik}$ ,  $(\mathcal{E}^4)_{ij}(\mathcal{E}^2)_{ik}$  and  $(\mathcal{E}^3)_{ij}(\mathcal{E}^3)_{ik}$  in (S28). To calculate the expectations of these terms, we consider the expression for the sixth power of (S27) in terms of the  $\Phi_{ij}$  terms. In Sections IC 1 to IC 4, we describe the method of calculating the expectations of each of the terms in (S28).

### 1. Calculating $E((\mathcal{E}^6)_{ij})$

Only terms in  $(\mathcal{E}^6)_{ij}$  involving products of certain  $\Phi_{ij}$  terms have nonzero expectation, such as  $\Phi_{12}^2 \Phi_{13}^2 \Phi_{23}^2$  which is the product of the square of three  $\Phi_{ij}$  terms that involve mutually uncorrelated variables. As another example, terms of the form  $\Phi_{ij}^4 \Phi_{ik}^2$  for  $j \neq k$  also has nonzero expectation. Another term in  $(\mathcal{E}^6)_{ij}$  with nonzero expectation is  $\Phi_{ij}^6$ . To count the number of terms of each form, we consider in Table I below the set of all forms in which the terms having nonzero expectation can take. Let  $A$ ,  $B$  and  $C$  denote the  $\Phi_{ij}$  matrices with variables that are all mutually uncorrelated when  $\rho \neq 0$  e.g.  $A = \Phi_{12}$ ,  $B = \Phi_{13}$  and  $C = \Phi_{23}$ , we have that

$A^2 B^2 C^2$	$A^4 B^2$	$A^6$
$\Phi_{ij}^2 \Phi_{ik}^2 \Phi_{jk}^2$	$\Phi_{ij}^4 \Phi_{ik}^2$	$\Phi_{ij}^6$
$\Phi_{ij}^2 \Phi_{ik}^2 \Phi_{il}^2$	$\Phi_{ij}^4 \Phi_{jk}^2$	
$\Phi_{ij}^2 \Phi_{ik}^2 \Phi_{kl}^2$	$\Phi_{ij}^4 \Phi_{kl}^2$	
$\Phi_{ij}^2 \Phi_{jk}^2 \Phi_{kl}^2$		
$\Phi_{ij}^2 \Phi_{ik}^2 \Phi_{jl}^2$		
$\Phi_{ij}^2 \Phi_{jk}^2 \Phi_{jl}^2$		
$\Phi_{ij}^2 \Phi_{jk}^2 \Phi_{il}^2$		

TABLE I: Set of all forms of different terms of  $\mathcal{E}^6$  which have nonzero expectations. We specifically do not allow any pair of indices to be equal i.e.  $i \neq j$ ,  $j \neq k$ . The first column ( $A^2 B^2 C^2$ ) involves products of 3 different matrices that contain mutually uncorrelated variables, while the second column ( $A^4 B^2$ ) involves products of 2 different matrices that contain mutually uncorrelated variables.  $i$  is assumed to be the free index throughout Section IC, with all other indices dummy indices.

Since matrix multiplication is not commutative, we now consider the set of all permutations of each entry of Table I above. First, we seek the set of all permutations of terms of each form that gives rise to a nonzero sum of first row (first row sum) (we take the first row  $i = 1$  W.L.O.G).  $\Phi_{ij}^2 \Phi_{ik}^2 \Phi_{jk}^2$  contains 6 permutations that give rise to a nonzero first row sum. The expectation of the first row sum of each matrix of this form (i.e expectation of the first row sum of  $\Phi_{12} \Phi_{13} \Phi_{23}$ ) is  $\rho^3$ . Since two indices ( $j$  and  $k$ ) are summed over, there exists  $(n-1)(n-2)$  terms in the sum. There exists 6 permutations with nonzero first row sums, but three of these 6 permutations are double countings of the other three. The expectation of  $\Phi_{ij}^2 \Phi_{ik}^2 \Phi_{jk}^2$  is thus  $3(n-1)(n-2)\rho^3$ .

$\Phi_{ij}^2 \Phi_{ik}^2 \Phi_{il}^2$  contains 2 distinct permutations that give rise to nonzero first row sum, and with 3 indices summed over, there are  $((n-1)^3 - (n-1)^2 - 2(n-1)(n-2))$  terms in the sum. Subtraction of  $(n-1)^2 + 2(n-1)(n-2)$  from  $(n-1)^3$  is to ensure no double countings in the sum over 3 indices. Since the expectation of the first row sum of each matrix of this form is also  $\rho^3$ , the expectation of  $\Phi_{ij}^2 \Phi_{ik}^2 \Phi_{il}^2$  is thus  $2((n-1)^3 - (n-1)^2 - 2(n-1)(n-2))\rho^3$ . The expectation of each entry of Table I is deduced by following these steps.

1. Checking the number of permutations of each entry of Table I that has a nonzero sum of (first) row. We do this for the first row if we set our dummy index  $i$  to 1 W.L.O.G. Check if any pair of rows are double countings of each other.
2. Calculating the expectation of the first row sum of each permutation that has a nonzero first row sum.
3. Count the number of terms in the sum over its set of dummy indices. We specifically do not allow any index to equal each other, not even the free index.
4. Check if any terms in the sums over its dummy indices are double counted by relabelling dummy indices. If there are double countings, subtract the number of double counted terms from the quantity deduced in 3. For example, if summing over 2 indices and we specifically do not allow any index to equal each other, then there are  $(n-1)^2 - (n-1)$  terms, since  $(n-1)^2$  terms are summed over and  $(n-1)$  of them are double counted.

Finally we take the product of all quantities deduced in 1. to 3. above to give the expectation of each entry of Table I. Repeating this procedure for all entries of Table I and summing, we find that

$$E((\mathcal{E}^6)_{ij}) = (n-1)(n-2) + (n-1)(9\rho + 6\rho^3) + 6(n-1)(n-2)\rho(1+2\rho^2) + 3(n-1)(n-2)\rho^3 + 5((n-1)^3 - (n-1)^2 - 2(n-1)(n-2))\rho^3 \quad (\text{S30})$$

If  $A$  has a connectance  $C$  and  $a_{ij}$  and  $a_{ji}$  are sampled from a bivariate distribution, then they are both nonzero with probability  $C$ , and so we have

$$E((\mathcal{E}^6)_{ij}) = (n-1)(n-2)C^3 + (n-1)(9\rho + 6\rho^3)C + 6(n-1)(n-2)\rho(1+2\rho^2)C^2 + 3(n-1)(n-2)\rho^3C^3 + 5((n-1)^3 - (n-1)^2 - 2(n-1)(n-2))\rho^3C^3 \quad (\text{S31})$$

### 2. Calculating $E((\mathcal{E}^5)_{ij}\mathcal{E}_{ik})$

Now we seek to find  $E((\mathcal{E}^5)_{ij}\mathcal{E}_{ik})$ . Table II shows the set of all forms in which the terms of  $(\mathcal{E}^5)_{ij}\mathcal{E}_{ik}$  having nonzero expectation can take.

$A^2B^2C^2$	$A^4B^2$	$A^6$
$(\Phi_{ij}^2\Phi_{jk}^2\Phi_{ik})\Phi_{ik}$	$(\Phi_{ij}^4\Phi_{ik})\Phi_{ik}$	$(\Phi_{ij}^5)\Phi_{ij}$
$(\Phi_{ij}^2\Phi_{ik}^2\Phi_{il})\Phi_{il}$	$(\Phi_{ij}^2\Phi_{ik}^3)\Phi_{ik}$	
$(\Phi_{ij}^2\Phi_{jk}^2\Phi_{jl})\Phi_{ij}$	$(\Phi_{ij}^3\Phi_{jk}^2)\Phi_{ij}$	
$(\Phi_{ij}^2\Phi_{jk}^2\Phi_{il})\Phi_{il}$	$(\Phi_{ij}^2\Phi_{jk}^4)\Phi_{ij}$	
$(\Phi_{ij}^2\Phi_{ik}^2\Phi_{jl})\Phi_{ij}$		
$(\Phi_{ij}^2\Phi_{ik}^2\Phi_{kl})\Phi_{ij}$		

TABLE II: Set of all forms of different terms of  $(\mathcal{E}^5)_{ij}\mathcal{E}_{ik}$  which have nonzero expectations. Here, all the  $\Phi_{ij}$  matrices inside the brackets represent matrices that comprise the term  $(\mathcal{E}^5)_{ij}$  and the matrix outside the brackets represent the  $\Phi_{ij}$  matrices that comprise  $\mathcal{E}_{ik}$ .

Next, we repeat step 1. detailed in the page above, but only for the terms inside the brackets. This gives  $(\mathcal{E}^5)_{ij}$ . After that, multiply the first row sums of all matrices with nonzero first row sum by the first row sum of the  $\Phi$  outside the bracket. In other words, multiplying  $(\mathcal{E}^5)_{ij}$  with  $\mathcal{E}_{ik}$ . We next calculate the expectation of this quantity. Then we repeat step 3 and 4. We find that

$$E((\mathcal{E}^5)_{ij}\mathcal{E}_{ik}) = 2(n-1)(n-2)(1+2\rho^2) + 5(3\rho^2(n-1)(n-2)) + (n-1)(n-2)\rho + 5((n-1)^3 - (n-1)^2 - 2(n-1)(n-2))\rho^2 + (n-1)(3+12\rho^2) \quad (\text{S32})$$

and if  $A$  has connectance  $C$  with  $a_{ij}$  and  $a_{ji}$  sampled from a bivariate distribution, then we have

$$E((\mathcal{E}^5)_{ij}\mathcal{E}_{ik}) = 2(n-1)(n-2)(1+2\rho^2)C^2 + 4(3\rho^2(n-1)(n-2))C^2 + (3\rho^2(n-1)(n-2))C^3 + (n-1)(n-2)\rho C^3 + 5((n-1)^3 - (n-1)^2 - 2(n-1)(n-2))\rho^2C^3 + (n-1)(3+12\rho^2)C \quad (\text{S33})$$

### 3. Calculating $E((\mathcal{E}^4)_{ij}(\mathcal{E}^2)_{ik})$

Now we seek to find  $E((\mathcal{E}^4)_{ij}(\mathcal{E}^2)_{ik})$ . Table III shows the set of all forms in which the terms of  $(\mathcal{E}^4)_{ij}(\mathcal{E}^2)_{ik}$  having nonzero expectation can take.

$A^2B^2C^2$	$A^4B^2$	$A^6$
$(\Phi_{ij}^2\Phi_{jk}^2)(\Phi_{ik}^2)$	$(\Phi_{ij}^2\Phi_{ik}^2)(\Phi_{ij}^2)$	$(\Phi_{ij}^4)(\Phi_{ij}^2)$
$(\Phi_{ij}\Phi_{ik}\Phi_{il}^2)(\Phi_{ij}\Phi_{ik})$	$(\Phi_{ij}^2\Phi_{jk}^2)(\Phi_{ij}^2)$	
$(\Phi_{ij}\Phi_{ik}\Phi_{jk}^2)(\Phi_{ij}\Phi_{ik})$	$(\Phi_{ij}^3\Phi_{ik})(\Phi_{ij}\Phi_{ik})$	
$(\Phi_{ij}\Phi_{ik}\Phi_{jl}^2)(\Phi_{ij}\Phi_{ik})$	$(\Phi_{ij}^3\Phi_{jk})(\Phi_{ij}\Phi_{jk})$	
$(\Phi_{ij}\Phi_{ik}\Phi_{kl}^2)(\Phi_{ij}\Phi_{ik})$	$(\Phi_{ij}\Phi_{jk}^3)(\Phi_{ij}\Phi_{jk})$	
$(\Phi_{ij}\Phi_{jk}\Phi_{ik}^2)(\Phi_{ij}\Phi_{jk})$	$(\Phi_{ij}^4)(\Phi_{ik}^2)$	
$(\Phi_{ij}\Phi_{jk}\Phi_{il}^2)(\Phi_{ij}\Phi_{jk})$		
$(\Phi_{ij}\Phi_{jk}\Phi_{jl}^2)(\Phi_{ij}\Phi_{jk})$		
$(\Phi_{ij}\Phi_{jk}\Phi_{kl}^2)(\Phi_{ij}\Phi_{jk})$		
$(\Phi_{ij}^2\Phi_{jk}^2)(\Phi_{il}^2)$		

TABLE III: Set of all forms of different terms of  $(\mathcal{E}^4)_{ij}(\mathcal{E}^2)_{ik}$  with nonzero expectations. Here, all the  $\Phi_{ij}$  matrices inside the left bracket represent those that comprise the  $(\mathcal{E}^4)_{ij}$  term and all the  $\Phi_{ij}$ s in the right bracket represents all those in the  $(\mathcal{E}^2)_{ik}$  term.

Now, it is necessary to seek the set of all  $(\mathcal{E}^4)_{ij}(\mathcal{E}^2)_{ik}$  such that both  $(\mathcal{E}^4)_{ij}$ s and  $(\mathcal{E}^2)_{ik}$ s have nonzero first row sums. In other words, all the entries in Table III in which both their left and right brackets have nonzero first row sums. To do this, we repeat step 1 for both the left and right brackets of each entry of table III, discarding any permutations of matrices in each bracket that have zero first row sums. Next, calculate the expectation of the product of the first row sum of the left bracket and the first row sum of the right bracket. Finally, repeat steps 3. and 4. We find that

$$\begin{aligned}
E((\mathcal{E}^4)_{ij}(\mathcal{E}^2)_{ik}) &= 4(n-1)(n-2)\rho(1+2\rho^2) + 8\rho(n-1)(n-2) \\
&\quad + 3\rho((n-1)^3 - (n-1)^2 - 2(n-1)(n-2)) + (n-1)(n-2)\rho^3 + (n-1)(n-2)\rho^2 \\
&\quad + 2((n-1)^3 - (n-1)^2 - 2(n-1)(n-2))\rho^3 + (n-1)(9\rho + 6\rho^3)
\end{aligned} \tag{S34}$$

and if  $A$  has connectance  $C$  with  $a_{ij}$  and  $a_{ji}$  sampled from a bivariate distribution, then we have

$$\begin{aligned}
E((\mathcal{E}^4)_{ij}(\mathcal{E}^2)_{ik}) &= 4(n-1)(n-2)\rho(1+2\rho^2)C^2 + 6\rho(n-1)(n-2)C^2 + 2\rho(n-1)(n-2)C^3 \\
&\quad + 3\rho((n-1)^3 - (n-1)^2 - 2(n-1)(n-2))C^3 + (n-1)(n-2)\rho^3C^3 + (n-1)(n-2)\rho^2C^3 \\
&\quad + 2((n-1)^3 - (n-1)^2 - 2(n-1)(n-2))\rho^3C^3 + (n-1)(9\rho + 6\rho^3)C
\end{aligned} \tag{S35}$$

Now, we find  $E((\mathcal{E}^3)_{ij}(\mathcal{E}^3)_{ik})$ . Since  $(\mathcal{E}^3)_{ij}(\mathcal{E}^3)_{ik}$  involves the product of two terms that contain a third power of  $\mathcal{E}$ , each one of which has a range of permutations that give rise to nonzero first row,  $(\mathcal{E}^3)_{ij}(\mathcal{E}^3)_{ik}$  will have more permutations that give nonzero first row. For instance, the first  $(\mathcal{E}^3)_{ij}$  can contain a product of either two or three different  $\Phi_{ij}$ s. We therefore follow an alternative set of steps.

1. Find the set of all permutations of the tuples  $(1, 2, 3, 1, 2, 3)$  and  $(1, 1, 1, 1, 2, 2)$ . Each number in the tuple represents a distinct  $\Phi_{ij}$  matrix e.g. 1 representing  $\Phi_{ij}$ , 2 for  $\Phi_{ik}$ , 3 for  $\Phi_{il}$ . Tuple  $(1, 2, 3, 1, 2, 3)$  represents the order of products of three distinct matrices ( $A^2B^2C^2$ ) while  $(1, 1, 1, 1, 2, 2)$  represents the order of products of two distinct matrices ( $A^4B^2$ ). The permutations of each of these tuples should be expressed as a table.
2. Split the tables of permutations found in step 1. into two tables by separating columns 1 to 3 and 4 to 6. In each of these two tables, discard any repeated rows if any. The table containing columns 1 to 3 represents the set of all permutations of  $(\mathcal{E}^3)_{ij}$  and the table containing columns 4 to 6 represents the set of all permutations of  $(\mathcal{E}^3)_{ik}$ .
3. Check which rows of both tables represent permutations that give nonzero first row sum in BOTH  $(\mathcal{E}^3)_{ij}$  and  $(\mathcal{E}^3)_{ik}$ .
4. Repeat Steps 3 and 4 in the list above (S30).

#### 4. Calculating $E((\mathcal{E}^3)_{ij}(\mathcal{E}^3)_{ik})$

The entries of Table IV represents the set of all  $\Phi_{ij}$  matrices that comprise the  $(\mathcal{E}^4)_{ij}(\mathcal{E}^2)_{ik}$ s which have nonzero expectations.

$A^2B^2C^2$	$A^4B^2$	$A^6$
$\Phi_{ij}\Phi_{ik}\Phi_{il}$	$\Phi_{ij}\Phi_{ik}$	$\Phi_{ij}$
$\Phi_{ij}\Phi_{ik}\Phi_{jk}$	$\Phi_{ij}\Phi_{jk}$	
$\Phi_{ij}\Phi_{ik}\Phi_{jl}$		
$\Phi_{ij}\Phi_{jk}\Phi_{jl}$		
$\Phi_{ij}\Phi_{jk}\Phi_{kl}$		
$\Phi_{ij}\Phi_{ik}\Phi_{kl}$		

TABLE IV: Each entry of the table contains the set of  $\Phi_{ij}$  matrices that make up the  $(\mathcal{E}^4)_{ij}(\mathcal{E}^2)_{ik}$  with nonzero expectations. The column  $A^2B^2C^2$  are the set of products of three different  $\Phi_{ij}$  matrices that can give nonzero first row sums depending on the permutation.  $A^4B^2$  are the set of products of two different  $\Phi_{ij}$  matrices that can give nonzero first row sums, and  $A^6$  is the product of a one such matrix e.g.  $\Phi_{ij}^6$ .

Using the method outline immediately above, we find that

$$\begin{aligned}
E((\mathcal{E}^3)_{ij}(\mathcal{E}^3)_{ik}) &= 4\rho^2((n-1)^3 - (n-1)^2 - 2(n-1)(n-2)) + 2(n-1)(n-2)\rho^2 \\
&\quad + (n-1)(n-2)\rho^3 + (n-1)(n-2) + ((n-1)^3 - (n-1)^2 - 2(n-1)(n-2)) \\
&\quad + 4(n-1)(n-2)3\rho^2 + 2(n-1)(n-2)(1+2\rho^2) + (n-1)(3+12\rho^2)
\end{aligned} \tag{S36}$$

and if  $A$  has connectance  $C$  with  $a_{ij}$  and  $a_{ji}$  sampled from a bivariate distribution, then we have

$$\begin{aligned}
E((\mathcal{E}^3)_{ij}(\mathcal{E}^3)_{ik}) &= 4\rho^2((n-1)^3 - (n-1)^2 - 2(n-1)(n-2))C^3 + 2(n-1)(n-2)\rho^2C^3 \\
&\quad + (n-1)(n-2)\rho^3C^3 + (n-1)(n-2)C^3 + ((n-1)^3 - (n-1)^2 - 2(n-1)(n-2))C^3 \\
&\quad + 4(n-1)(n-2)3\rho^2C^2 + 2(n-1)(n-2)(1+2\rho^2)C^2 + (n-1)(3+12\rho^2)C
\end{aligned} \tag{S37}$$

We can use (S30) to (S37) to calculate the expectation of (S28).

#### D. Accuracy of Analytical Prediction

The analytical prediction of  $P_{feas}(\gamma, \rho)$  remains accurate up to  $|\rho| = 0.5$  for  $n = 100$  and  $|\rho| = 0.25$  for  $n = 25$ .

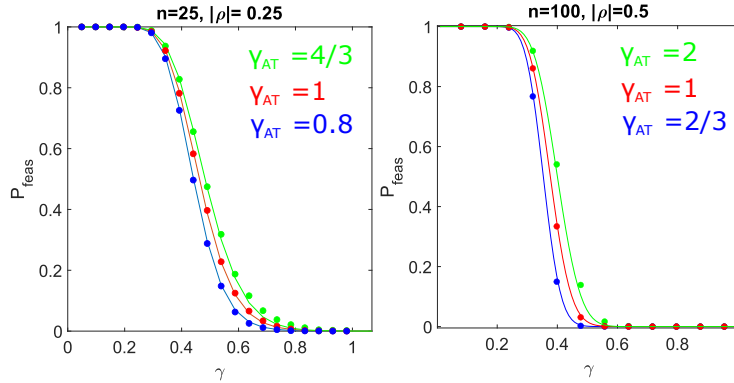


FIG. S1: Dots are numerical simulations of  $P_{feas}(\gamma, \rho)$ . Solid curves are analytical predictions of  $P_{feas}(\gamma, \rho)$  using  $E(x_i^*)$  approximated up to and including order  $\sigma^3$  and  $Var(x_i^*)$  up to and including order  $\sigma^6$ . The system has  $C = 1$ . Blue  $\rho < 0$ , red  $\rho = 0$  and green  $\rho > 0$ .  $\gamma_{AT}$  is the complexity above which linear stability is lost in the Allesina and Tang 2015 model. For any value of  $\rho$ , feasibility is lost at smaller complexities than linear stability in large systems.

We see from Figure S1 that feasibility is lost at a smaller complexity compared to linear stability. For systems with  $\rho < 0$ , feasibility is lost at a much smaller complexity compared to linear stability than systems with  $\rho > 0$ , implying that increasing the proportion of predator-prey interactions will have a more modest effect on stability than predicted by Allesina and Tang. Figure S2 plots numerical simulations of  $P_{feas}(\gamma, \rho)$  for the case where  $\rho = \pm 1$ . For the case where  $\rho = -1$ ,  $P_{feas}$  still decreases to 0 above a sufficiently large complexity even though the system is linearly stable for all complexities.

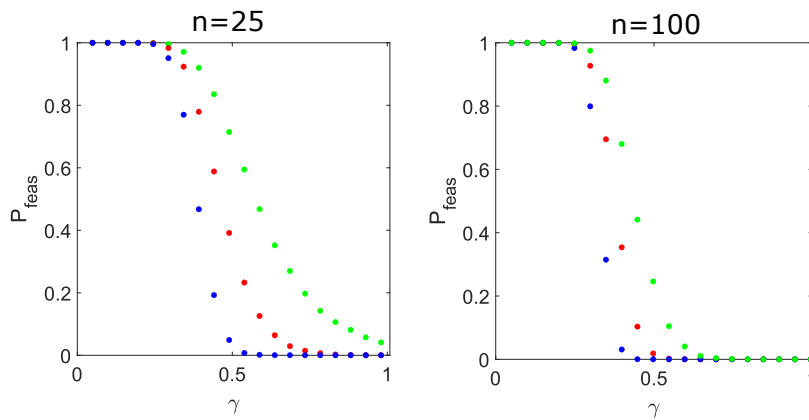


FIG. S2: Numerical simulations of  $P_{feas}(\gamma, \rho)$  for the case where  $|\rho| = 1$ . Analytical predictions break down for this magnitude of  $\rho$ , so only numerical simulations are included. The system has  $C = 1$ .

## II. PARAMETER REGIONS WHERE APPROXIMATION OF $Var(x_i^*)$ BEYOND ORDER $\sigma^6$ IS REQUIRED

In Figure S4, we show examples of plots in parameter regions where the approximation of  $P_{feas}(\gamma, \rho)$  breaks down. It is apparent from Figure S3 that for large magnitudes of  $\rho$ , the analytical approximation of  $Var(x_i^*)$  to order  $\sigma^6$  breaks down at a smaller value of  $\sigma$ . Since systems with a large negative  $\rho$  also has a higher  $P_{feas}$  at a given value of  $\sigma$ , the analytical prediction of  $P_{feas}(\gamma, \rho)$  becomes inaccurate before  $P_{feas}(\gamma, \rho)$  transitions to 0. These points indicate how the analytical approximation would break down given a sufficiently large negative  $\rho$ . We also show in Figure S4 that for systems such as  $n = 25$ , the analytical prediction of  $P_{feas}(\gamma, \rho)$  also breaks down for small  $C$ .

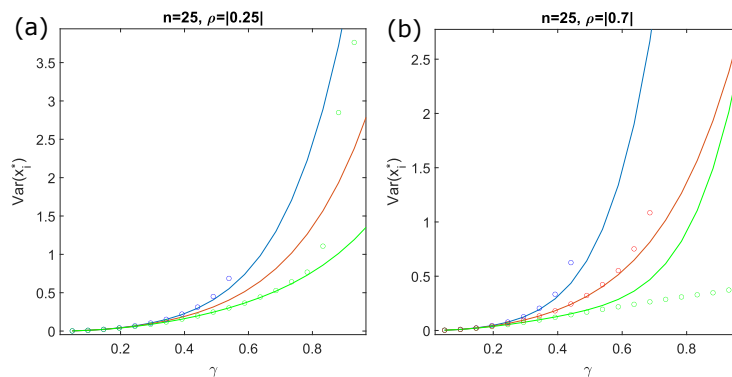


FIG. S3:  $Var(x_i^*)$  as a function of  $\gamma$  for systems with  $n = 25$ . Panel (a) is for system with  $|\rho| = 0.25$  and panel (b) for  $|\rho| = 0.7$ . It is evident from panel (b) that for large negative  $\rho$  such as  $\rho = -0.7$ , the analytical prediction of  $Var(x_i^*)$  breaks down at around  $\gamma = 0.5$ , which is a smaller value than for the case  $\rho = -0.25$  where the analytical prediction breaks down at a around  $\gamma = 0.8$ . For  $\rho = 0$  and  $\rho > 0$ , outliers in  $x_i^*$  begin to emerge above a sufficiently large  $\gamma$ , causing numerical data of  $Var(x_i^*)$  to become noisy.

In the right panel ( $n = 25$ ,  $\rho = -0.7$ ), the feasibility probability at value of  $\gamma$  at which the order  $\sigma^6$  approximation of  $Var(x_i^*)$  breaks down is 0.632, whereas in the left panel ( $n = 25$ ,  $\rho = -0.25$ ), this corresponding feasibility probability is 0.021. In Figure S4, we show that the analytical prediction of  $P_{feas}(\gamma, \rho)$  can break down if either  $\rho$  is sufficiently large or if  $C$  is sufficiently small for a fixed community size  $n$ .

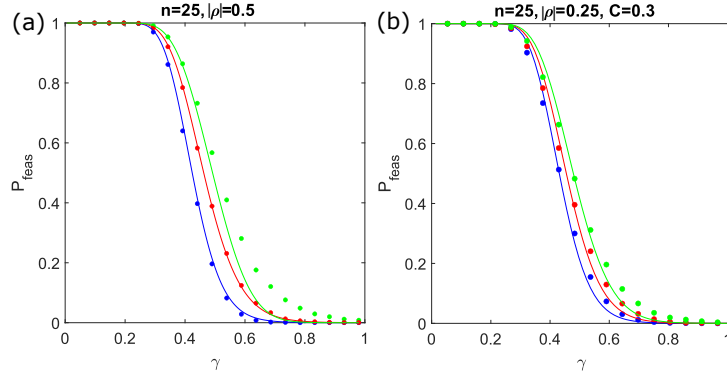


FIG. S4: (a) The analytical prediction of  $P_{feas}(\gamma, \rho)$  breaks down when  $\rho$  is sufficiently large and negative given a sufficiently small  $n$ . Here  $C = 1$ . (b) The analytical prediction of  $P_{feas}(\gamma, \rho)$  breaks down when  $C$  is sufficiently small.

It is worth noting that when  $\rho$  becomes sufficiently large and negative, the variance-covariance matrix ceases to be positive semi-definite if  $Var(x_i^*)$  is approximated up to order  $\sigma^6$ .

### III. ANALYTICAL PREDICTION OF FEASIBILITY PROBABILITY AS A FUNCTION OF COMPLEXITY

The analytical prediction of  $P_{feas}$  as a function of complexity  $\gamma$  is determined by integrating the joint density function of  $\mathbf{x}^*$  from  $x_i^* = 0$  to  $x_i^* = \infty$  for all  $i \in [1, n]$ . For systems of  $n \leq 25$ , this is done using the *mvncdf* command in MATLAB. For systems where  $n > 25$ , *mvncdf* is no longer applicable, therefore we obtain the analytical prediction of  $P_{feas}$  as a function of  $\gamma$  by reducing the multivariate normal integral to a single integral using the method detailed in [2]. The multivariate normal distribution function is given by

$$F_{\mathbf{X}}(\mathbf{X}) = \int_{-\infty}^{x_1} \dots \int_{-\infty}^{x_n} f_{\mathbf{X}}(\mathbf{X}, \Sigma^{\mathbf{X}}) d\mathbf{X} \quad (\text{S38})$$

where  $\Sigma^{\mathbf{X}}$  is the variance-covariance matrix of  $\mathbf{X}$ . Here  $\mathbf{X}$  is a random variable such that  $X_i = -x_i^*$ . Define  $y_i$  as a standardised normal random variable  $y_i = \frac{X_i - \mu_{X_i}}{\sigma_{X_i}}$ . If  $Corr(x_i^*, x_j^*)$  can be expressed in the form  $Corr(x_i^*, x_j^*) = b_i b_j$  where  $b_i, b_j \in \mathbb{R}$ , then  $F_{\mathbf{X}}(\mathbf{X})$  can be expressed as

$$F_{\mathbf{X}}(\mathbf{X}) = \int_{-\infty}^{\infty} \left\{ \prod_{i=1}^n \Phi\left(\frac{y_i - b_i u}{(1 - b_i^2)^{1/2}}\right) \right\} \phi(u) du \quad (\text{S39})$$

where  $\phi(u)$  is the density function of a standard normal random variable  $u$  and  $\Phi(v)$  denotes the cumulative distribution function of a standard normal random variable  $v$  [2]. The condition of feasibility  $\mathbf{x}^* > \mathbf{0}$  is equivalent to the condition that  $\mathbf{X} < \mathbf{0}$ . Since  $y_i = \frac{X_i - E(X_i)}{\sigma_{X_i}}$ , the condition that  $X_i < 0$  is equivalent to the condition that  $y_i < -E(X_i)/\sigma_{X_i}$  and thus  $y_i < E(x_i^*)/\sigma_{x_i^*}$ . In our analytical prediction of  $P_{feas}$ , we have that  $y_i = \frac{E(x_i^*)}{\sqrt{Var(x_i^*)}}$  and  $b_i = \frac{\sqrt{Cov(x_i^*, x_j^*)}}{\sqrt{Var(x_i^*)}}$ . In other words,  $P_{feas}$  is the expression you get by plugging these expressions for  $y_i$  and  $b_i$  into (S39). The integral (S39) is also applicable for  $Cov(x_i^*, x_j^*) < 0$ , however the integrand is complex [2]. As a result, we approximated  $P_{feas}(\gamma, \rho)$  for the case  $\rho < 0$  by numerically integrating (S39) using the *NIntegrate* command in mathematica. The lower and upper limits of this integral are set to -20 and 20 respectively. This numerical integral works well since the imaginary part is of magnitude  $10^{-18}$  and the real part matches the numerical simulations of  $P_{feas}(\gamma, \rho)$  closely, as can be seen in Figure S1.

### IV. OBTAINING NUMERICAL SIMULATIONS OF FEASIBILITY PROBABILITY

In fully connected systems  $C = 1$ , we obtained 10000 numerical solutions of  $\mathbf{x}^*$  by doing 10000 successive runs of the GLV equation (Eq. (3) in main text). This step is repeated for each value of  $\sigma$ ,  $n$  and  $\rho$  I considered. The feasibility probability is calculated by calculating the fraction of numerical solutions of  $\mathbf{x}^*$  out of the 10000 that



contain all non-negative entries. For predator-prey, mutualistic and competitive interactions ( $\rho \neq 0$ ), the off diagonal elements  $a_{ij}$  and  $a_{ji}$  of  $\mathbf{A}$  are sampled from a bivariate normal distribution where  $\text{Corr}(a_{ij}, a_{ji}) = \rho$ ,  $E(a_{ij}) = 0$  and  $\text{Var}(a_{ij}) = 1$ . For the systems with random interaction structure ( $\rho = 0$ ), all off-diagonal elements of  $\mathbf{A}$  are sampled independently from an  $N(0, \sigma^2)$  distribution.

When considering sparsely connected matrices ( $C < 1$ ), we exclude such matrices  $\mathbf{A}$  that contain disconnected components. In particular, we obtain 10000 realisations of  $\mathbf{x}^*$  which correspond to sparse interaction matrices that contain no disconnected components. The off diagonal elements  $a_{ij}$  and  $a_{ji}$  are 0 with probability  $1 - C$  and sampled from a bivariate normal distribution where  $\text{Corr}(a_{ij}, a_{ji}) = \rho$ ,  $E(a_{ij}) = 0$  and  $\text{Var}(a_{ij}) = 1$  with probability  $C$ . Even in the case where  $\rho = 0$ , we sample the off diagonal elements of  $\mathbf{A}$  from the same bivariate distribution rather than independently from an  $N(0, \sigma^2)$  distribution with probability  $C$ , as was the case of May [1]. We do this because for systems where  $C < 1$ , sampling  $a_{ij}$  and  $a_{ji}$  from a bivariate normal distribution with  $\rho = 0$  would give a different  $P_{feas}$  to sampling all off-diagonal elements of  $\mathbf{A}$  independently as May did. However in the case where  $C = 1$ , sampling  $a_{ij}$  and  $a_{ji}$  from a bivariate normal distribution with  $\rho = 0$  gives the same feasibility probability as when all off-diagonal elements of  $\mathbf{A}$  are sampled independently from an  $N(0, \sigma^2)$  distribution.

## V. ANALYTICAL PREDICTION FOR SPARSELY CONNECTED SYSTEMS

Empirical ecological networks may be sparsely connected [3], so it would be useful to generalise our feasibility calculations to account for connectance  $C$ . Recent work by Akjouj and Najim [4] have shown that in sparse random GLV systems with block structure,  $P_{feas}$  also exhibits a rapid transition to 0 above a critical interaction strength, hinting that it could be viable to generalise Stone's analytical prediction to account for  $C$ . In this section, we demonstrate the success of this generalisation by providing an example in Figure S5. In Figure S5, we show that for a system with  $n = 100$ , analytical predictions for  $P_{feas}(\gamma, \rho)$  remain highly accurate even in systems with connectance as low as  $C = 0.3$ .

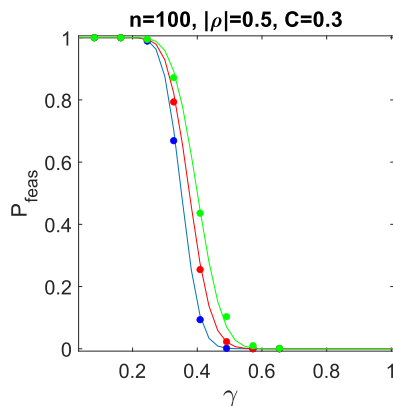


FIG. S5: We show that the analytical prediction of feasibility probability as a function of complexity [5] can be generalised for  $C$  as well as  $\rho$  (i.e.  $P_{feas}$  as a function of  $\gamma$  where  $\gamma = \sigma\sqrt{(n-1)C}$ ). All labels and parameters for this figure are the same as that of Figure 3 right, except  $C = 0.3$ . Our analysis of  $n$  species systems concerns systems comprising  $n$  species that interact as a single unit, so interaction matrices of  $C < 1$  that contain disconnected components are excluded from our analysis (see Supplemental Information IV).

By comparing the analytical and numerical data in Figure S5 with those of Figure S1, we see that the system with  $C = 0.3$  shows an almost identical feasibility profile with a system of  $C = 1$ . In other words, we get the same value of  $P_{feas}$  for a given value of  $\gamma_M$  in both systems. This implies that increasing  $\sigma$  and decreasing  $C$  to give the same complexity has negligible effect on the feasibility profile.

## VI. EFFECT OF $\rho$ ON OUTLIER EIGENVALUE

This section shows the effect of  $\rho$  on the stability of GLV systems by looking at how the outlier eigenvalue of  $J$  changes with  $\rho$ . It also shows that the abundance of the least abundant species is a good predictor of the outlier eigenvalue of  $J$ , and thus its stability.

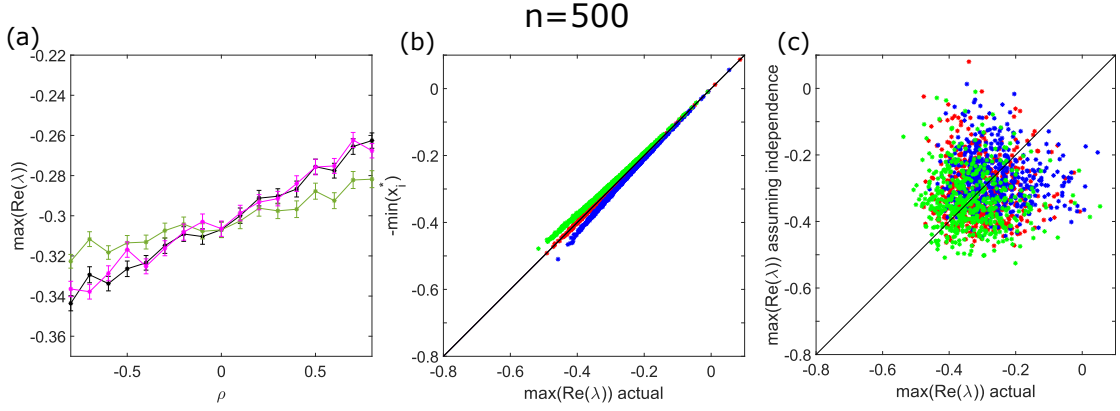


FIG. S6: Panel (a) shows the effect of  $\rho$  on the outlier eigenvalue of  $J = \mathbf{x}^* A$ , averaged over 500 realisations. Black represents the outlier eigenvalue of the actual GLV Jacobian ( $\max(\text{Re}(\lambda))$  actual). Green represents the outlier eigenvalue approximated by the relation  $\max(\text{Re}(\lambda)) = -\min_{i \in \{1, n\}} x_i^*$  and pink is the outlier eigenvalue of  $J$  constructed by sampling  $\mathbf{x}^*$  and  $A$  independently. Error bars represent the standard error about the mean. Panel (b) plots  $-\min_{i \in \{1, n\}} x_i^*$  against  $\max(\text{Re}(\lambda))$  actual for 500 realisations of the GLV system, with  $\gamma = 0.01\sqrt{499}$ . Blue  $\rho = 0.7$ , red  $\rho = 0$  and green  $\rho = -0.7$ . Black line is the line on which  $\max(\text{Re}(\lambda)) = -\min_{i \in \{1, n\}} x_i^*$ . Panel (c) plots  $\max(\text{Re}(\lambda))$  actual against that of  $J$  constructed by sampling  $\mathbf{x}^*$  independently of  $A$ .

Panel (a) shows that the outlier of the Jacobian constructed by sampling  $x^*$  independently of  $A$  (Grilli's assumption) correctly captures the qualitative effect of  $\rho$  on stability. Although it is shown in panel (c) that constructing the Jacobian by adopting Grilli's assumption fails to accurately calculate the outlier eigenvalue of each Jacobian. Panel (b) shows that  $-\min_{i \in \{1, n\}} x_i^*$  is a highly accurate predictor of stability of the GLV system corresponding to a given realisation of  $A$ , since most green markers sit close to the diagonal line. Notice that for systems where  $\rho > 0$ , the markers lie below the diagonal line. This implies that the stability is marginally overestimated by the relation  $\max(\text{Re}(\lambda)) = -\min_{i \in \{1, n\}} x_i^*$  and for  $\rho < 0$ , this relation underestimates the stability slightly. Since  $\text{Corr}(\max(\text{Re}(\lambda)), -\min_{i \in \{1, n\}} x_i^*) = 0.9999$ , when  $\rho = 0$   $\text{Corr}(\max(\text{Re}(\lambda)), -\min_{i \in \{1, n\}} x_i^*) = 0.9996$  when  $\rho = -0.7$  and  $\text{Corr}(\max(\text{Re}(\lambda)), -\min_{i \in \{1, n\}} x_i^*) = 0.9995$  when  $\rho = 0.7$ ,  $-\min_{i \in \{1, n\}} x_i^*$  is an accurate predictor of stability for all regimes of  $\rho$ . It is of note that for large magnitudes of  $\rho$ ,  $-\min_{i \in \{1, n\}} x_i^*$  becomes a poor predictor of the outlier eigenvalue of  $J$  statistically, and thus a poor estimator of stability.

For smaller  $n$  systems, the accuracy of  $-\min_{i \in \{1, n\}} x_i^*$  at predicting the outlier eigenvalue of  $J$  is reduced to such an extent that it ceases to accurately predict the effect of  $\rho$  on resilience.

- 
- [1] Robert M May. Will a large complex system be stable? *Nature*, 238(5364):413–414, 1972.
  - [2] Robert N Curnow and Charles W Dunnett. The numerical evaluation of certain multivariate normal integrals. *The Annals of Mathematical Statistics*, pages 571–579, 1962.
  - [3] Mark R Gardner and W Ross Ashby. Connectance of large dynamic (cybernetic) systems: critical values for stability. *Nature*, 228(5273):784–784, 1970.
  - [4] Imane Akjouj and Jamal Najim. Feasibility of sparse large lotka-volterra ecosystems. *arXiv preprint arXiv:2111.11247*, 2021.
  - [5] Lewis Stone. *Some problems of community ecology: processes, patterns and species persistence in ecosystems*. PhD thesis, Monash University, 1988.